First measurements of a scintillator based Fast-Ion Loss Detector near the ASDEX Upgrade divertor[a)]

J. Gonzalez-Martin[1,3], J. Ayllon-Guerola[1,3], M. Garcia-Munoz[2,3], A. Herrmann[4], P. Leitenstern[4], P. De Marne[4], S. Zoletnik[5], A. Kovacsik[5], J. Galdon-Quiroga[2,3], J. Rivero-Rodriguez[1,3], M. Rodriguez-Ramos[2,3], L. Sanchis-Sanchez[2,3], J. Dominguez[1], ASDEX Upgrade Team[b)], and MST1 Team[c)]

[1]*Department of Mechanical and Manufacturing Engineering, University of Seville, C/Camino de los Descubrimientos s/n, Isla de la Cartuja, Seville, Spain*
[2]*Department of Atomic, Molecular and Nuclear Physics, Faculty of Physics, University of Seville, 41012 Seville, Spain*
[3]*CNA (U. Sevilla, CSIC, J. de Andalucia), Seville, Spain*
[4]*Max-Planck-Institut für Plasmaphysik, Garching, Germany*
[5]*Wigner RCP, Budapest, Hungary*

(Presented XXXXX; received XXXXX; accepted XXXXX; published online XXXXX)
(Dates appearing here are provided by the Editorial Office)

A new reciprocating scintillator based fast-ion loss detector (FILD) has been installed a few centimeters above the outer divertor of the ASDEX Upgrade tokamak and between two of its lower ELM mitigation coils. The detector head containing the scintillator screen, Faraday cup, calibration lamp and collimator systems are installed on a motorized reciprocating system that can adjust its position via remote control in between plasma discharges. Orbit simulations are used to optimize the detector geometry and velocity-space coverage. The scintillator image is transferred to the light acquisition systems outside of the vacuum via a lenses relay (embedded in a 3D-printed titanium holder) and an in-vacuum image guide. A Charge Couple Device (CCD) camera, for high velocity-space resolution, and an 8x8 channels Avalanche Photo Diode (APD) camera, for high temporal resolution (up to 2MHz), are used as light acquisition systems. Initial results showing NBI prompt losses velocity-space and fast-ion losses induced by an (2,1) neoclassical tearing mode (NTM) are presented.

I. INTRODUCTION

In magnetically confined fusion plasmas, fast-ion confinement is essential to assure device integrity and heating efficiency, especially in ITER and future fusion reactor with a large population of fusion-born alpha particles[1]. In present-days devices, scintillator-based Fast-Ion Loss Detectors (FILD)[2] are considered as one of the main diagnostics to study fast-ion loss mechanisms as they provide velocity-space measurements of escaping fast-ions with alfvénic temporal resolution.

Despite its unique capabilities, the fact that FILD can only provide local measurements, makes a stand-alone FILD insufficient while trying to fully characterize the losses produced by 3D magnetohydrodynamic (MHD) perturbations[3]. For that reason, different tokamaks have been equipped with more than one FILD[4-6] revealing the spatial dependency of fast-ion losses under different heating schemes, perturbative coils configurations[7] and MHD fluctuations[8]. Particularly, the ASDEX Upgrade (AUG) tokamak counted so far with a set of three FILDs, all of them above the midplane. Aiming to improve the poloidal coverage of this set, a new detector (labelled FILD5) has recently been installed in between two of the lower ELM mitigation coils, providing direct measurements of the losses a few centimetres above the lower outer divertor, which opens the possibility to study x-point fluctuations on NBI losses.

This document is organized as follows. A detailed description of the diagnostic setup (including probe head, velocity-space coverage, remotely-controlled reciprocating system, optics relay and DAQs) is given in section II. First measurements observed during the last experimental campaign (including NBI prompt losses and MHD induced fast-ion losses) are discussed in section III. Section IV summarizes the document and briefs forthcoming efforts.

II. DIAGNOSTIC SETUP

The design of this new FILD is based on the three already existing detectors. Escaping ions reaching the wall on their gyro-orbits enter the detector head through a small slit impinging a scintillator-coated plate, inducing light. The slit, together with the protection head, collimates incoming ions, so only desired orbits strike the scintillator plate. The two-dimensional pattern of the emitted light depends on the gyroradii and pitch-angle of the collimated trajectories while short decay time (490 ns) of the scintillating material (TG-Green) enables to identify fast-ion avalanches produced by high-frequency MHD phenomena.

[a)]Published as part of the Proceedings of the 22nd Topical Conference on High-Temperature Plasma Diagnostics (HTPD 2018) in San Diego, California, USA.
[b)]A. Kallenbach *et al*., Nucl. Fusion **53**, 102015 (2017)
[c)]H. Meyer *et al*., Nucl. Fusion **57**, 102014 (2017)

A. Detector head design and location

The graphite cup (diameter ~7cm) protecting sensitive components from heat and particle fluxes is D-shaped to maximize the number of fast-ions entering the scintillating chamber. The ion entrance aperture (0.5mm width, 2mm long and 10.5mm deep) is placed 5 mm away of the scintillator plate, whose position within the light acquisition systems can be determined lighting up a halogen lamp embedded on the head. To track the heat shield temperature, a thermocouple contacts the inner surface of the graphite cup. Additionally, a secondary plate has been implanted behind the scintillator plate, acting as a Faraday cup and allowing a complementary method for absolute measurements of fast-ion losses. A more detailed description of FILD probe heads can be found in [2].

To maintain the magnetic field lines lying on the scintillator plate and parallel to the collimator slit, the detector head is at 45 degrees with respect to the mid plane and 12 degrees around its own axis. It rests between B-coils IL3 and IL4 right above the divertor as shown in figure 1. When FILD is not being used, the probe head outermost surface remains sheltered by the two surrounding B-coil protection parts, which were milled to accommodate the diagnostic.

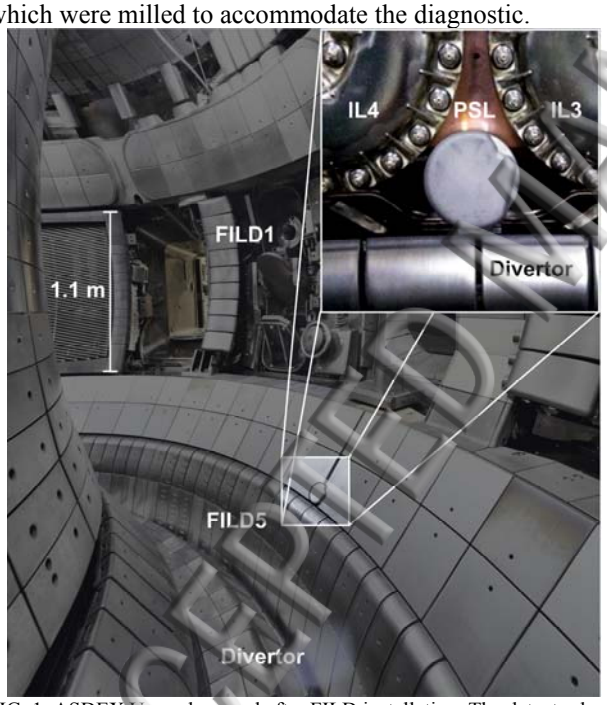

FIG. 1. ASDEX Upgrade vessel after FILD installation. The detector head can be spotted among the milled B-coil protection parts. The inset shows the FILD head during montage, surrounded by B-coils, divertor and PSL.

B. Velocity-space coverage

Full orbit simulations are used to optimize detector geometry and estimate velocity-space coverage depending on magnetic equilibrium[9]. Particles with gyroradius ranging from 2 to 8 centimetres and pitch angle from 20 to 80 degrees are initialized on the collimator slit. Trajectories are calculated backwards in time, identifying collisions with a 2D wall. Markers completing a total of three toroidal turns without colliding with the wall are considered as covered by FILD. Velocity-space is calculated for different FILD insertions, enabling us to identify the optimal measuring position. Figure 2 shows velocity-space coverage diagram calculated using the equilibrium reconstruction of a plasma discharge performed during last campaign.

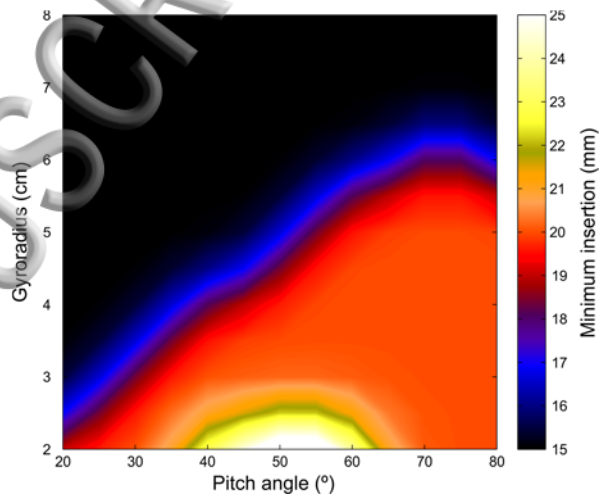

FIG. 2. Velocity-space coverage diagram for shot #34570 at 3.4s, showing full coverage for FILD outermost position. When FILD is inserted less than 15 mm, coverage is zero since the collimator slit is behind the wall.

C. FILD reciprocating system

In order to expose the collimator slit to fast-ion orbits, movement from the out-vessel driving unit needs to be transmitted to the off-axis rod which holds the probe head (figure 3). For this reason, a rotary feedthrough is coupled to a worm-gear by means of a 1-meter double-cardan joint along a radial port originally dedicated to the B-coils. The worm-gear transmits its linear movement to the off-axis rod via two crank shafts (one on each side of the detector). The movement of the off-axis rod is restricted by a set of 4x2 bearings, which are clamped to a holder armed with two in-vessel end-of-stroke electrical switches. Signals provided

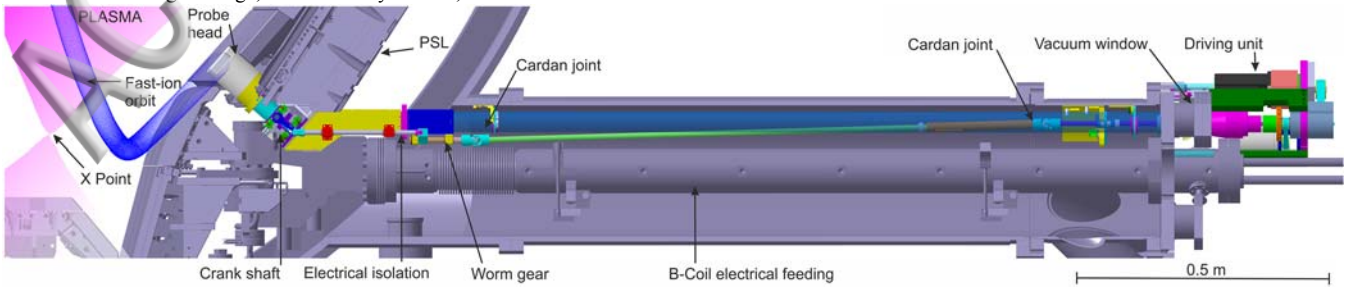

FIG. 3 Computer-aided design (CAD) view of the FILD system embedded on the AUG vessel. One can observe the in-vessel mechanical driving unit, including double-cardan joint, worm-gear, crank shaft and bearing set. Additionally, the electrically isolated case containing the lenses relay together with the pipe enclosing the image bundle are displayed.

by this switches are used by the Discharge Control System (DCS) to determine whether the programmed discharge is compatible with the current configuration of the FILDs.
The set of forefront mechanical elements is fastened to a metallic case which encloses part of the lenses relay. Since this case is fixed to the PSL, electrical insulations made of vacuum-compatible polymers such as Polyether Ether Ketone (PEEK)[10] and Vespel are used to contact components at vessel potential.

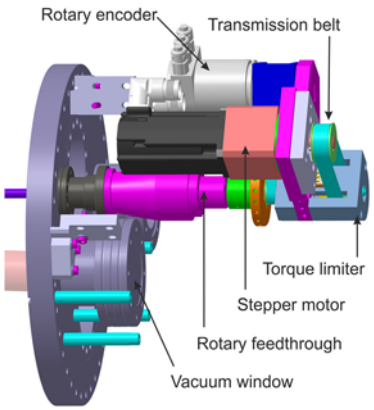

FIG. 4. Assembly of the different elements of the out-vessel remotely controlled driving unit (stepper motor, rotary encoder, transmission belt and torque limiter). Additionally, the antireflection-coated vacuum window can be spotted next to the driving unit.

To reach its outermost position, FILD head needs to move 25mm along its axis, which correspond to a total of 20 turns of the rotary feedthrough. The rotation of this element is provided by the out-vessel driving unit[11] (figure 4). It consists of a stepper motor (MICRON XTRUE 60), an absolute rotary encoder (PROFIBUS-DP class 2), a transmission belt and a spring torque limiter. The torque limiter connects the stepper motor and the rotary encoder protecting the rotary feedthrough. Comparing the rotary encoder signal with the embedded motor encoder allows identifying slipping caused by in-vessel worm gear clogging. Both the motor and the rotary encoder are controlled by a Programmable Logic Computer (PLC) S7 SIMATIC. The most sensitive elements such as the main PLC and the motor controller are placed in the transfer room so they are protected from the electric and magnetic fields that could harm them. The FILD operator can remotely communicate with the PLC using the human-machine interface system WinCC.

D. Optics relay and light acquisition systems

The light pattern emitted by the scintillating plate is transferred to the light acquisition systems outside of the vacuum via an in-vessel optics set. Four components can be distinguished. First, a 3D printed titanium body occupies all the room from 4cm to the scintillator plate until the end of the off-axis rod, holding a total of 8 lenses. This is needed to deviate the scintillating image through the off-axis rod. The titanium body was milled to accommodate the thermocouple case, calibration lamp and Faraday cup wires. Secondly, already inside the PSL-clamped case, a set of 2 mirrors is used to deflect the light towards the radial port. Then, a set of 4 lenses hold by an electrically insulated structure, projects the light on an in-vessel coherent image guide. The image guide consists on 40x50 quartz-made optic fibers, whose transmission is not harmed by the neutron radiation. Finally, the light goes through an anti-reflection coated vacuum window which filters out light outside the bandwidth emitted by the scintillator.

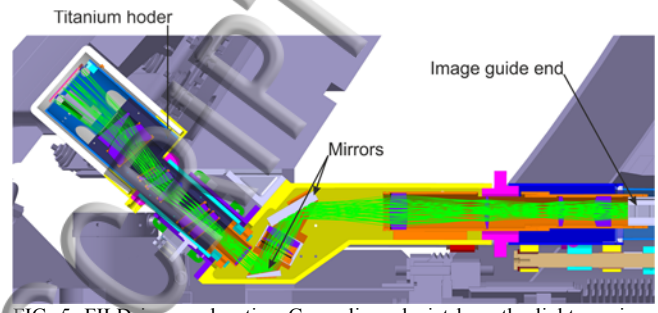

FIG. 5. FILD in-vessel optics. Green lines depict how the light coming from the scintillator rod is conducted towards the radial port and projected onto the image guide end.

The light beam coming from the vacuum window is diverted into two light acquisition systems via a drilled mirror which acts as an optimized beam splitter. The light acquisition systems are a Charge Couple Device (CCD)[12] camera, for high velocity-space resolution, and an 8x8 channels Avalanche Photo Diode (APD)[13] camera, for high temporal resolution (up to 2MHz).
The APD camera replaces Photo Multiplier Tubes (PMTs) used in former FILDs. It can be directly installed near the vessel, saving the long fiber bundle needed by PMTs to carry the light from the torus hall to the transfer room. The detector chip of the APD camera is covered by an array of small lenses to focus all the incoming light into the sensitive regions of the detector. The APD camera communicates with a dedicated server in the control room via a 10Gbits optic connection. Additionally, it receives an interlock trigger signal and a clock signal of 2MHz.
The CCD camera 2m ethernet cable is insulated by a copper mesh against Ion Cyclotron Resonance Frequency (ICRF) cross-talk. Its signal is sent to the control room via optic wire using a data converter. Once in the control room, the signal is transferred to a Linux PC using a PCI card. When the DCS communicates the beginning of the discharge via an interlock signal, the PC start recording with a sample rate of 50 frames per second.

III. FIRST MEASSUREMENTS

The new FILD has been operating during the last AUG experimental campaign. After measuring prompt and MHD-induced fast-ion losses in dedicated experiments, it was successfully used in other scenarios where FILDs normally have complications (e.g. upper single null). In this article, the most conspicuous results are shown as proof of principle, leaving the rest of the observations for forthcoming analysis.

A. NBI prompt losses

The ASDEX Upgrade tokamak has excellent qualities for fast particle experiments. Its heating system consists of 6 MW of IRCH, 2 MW of ECRH and 20 MW of NBI, distributed among 8 different sources at 60/93 keV with different injection geometries, being the 93 keV beams right above the new FILD.

Part of the NBI injected ions are born in unconfined orbits, depending on magnetic equilibrium, kinetic profiles and applied beam, these particles (also known as prompt losses) are usually observed by FILD detectors.

Figure 6 shows the heating power time trace of NBI injector Q8 matching the scintillating light recorded by APD camera channel 8 during a discharge with a toroidal current of I_p = 0.45MA and a toroidal field of B_t = 2.4T. This confirms that light emitted by the scintillator plate is produced by fast-ion injected by the NBI source.

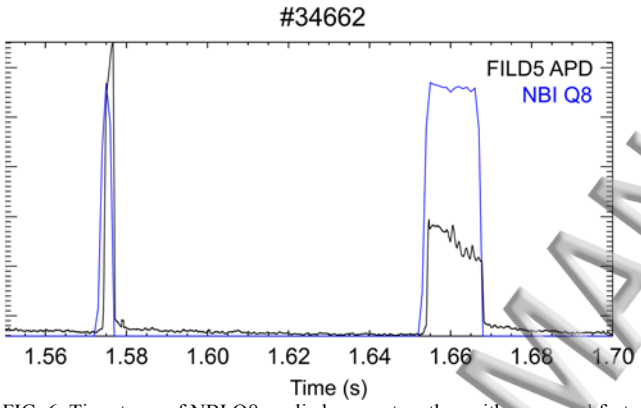

FIG. 6. Time trace of NBI Q8 applied power together with measured fast-ion losses with APD channel 8 corresponding to energy E~93keV and pitch angle α~45º.

Besides, the velocity-space of the escaping ions can be inferred as follows. FILDSIM[14] simulations are used to build a strike map containing the synthetic gyroradius and pitch angle distribution on the scintillator plate. The resulting strike map depends on the collimator slit dimensions and magnetic field vector near the probe-head. The halogen lamp embedded in the graphite head is used to obtain a backlighted image of the scintillator plate which helps to overlay the strike map on its correct position. The losses are observed to be centred around Larmor radii ρ_L ~ 2.7cm corresponding to deuterium ions injected at 93 keV (given the magnetic field at FILD position $|\boldsymbol{B}|$ = 2.3T). Moreover, the strike map is used for CCD frame triangulation, to obtain the image shown in figure 7b, allowing an easier comparison among experimental data and simulations.

B. MHD induced fast-ion losses

During 4 MW ICRH heated discharges, with a plasma current of I_p = 0.7MA and a toroidal magnetic field of B_t = 2.5T, a neoclassical tearing mode (NTM) evolves as shown in figure 8 magnetic spectrogram. Analysis of Mirnov coils signals is used to calculate poloidal (m=2) and toroidal (n=1) mode numbers. Using electron cyclotron emission (ECE) fast measurements, the magnetic island is determined to be located at ρ_{pol}=0.6.

FILD APD camera adjacent channels show the same trace on the spectrogram during the saturated phase of the magnetic island, indicating coherent fast-ion losses produced by the NTM.

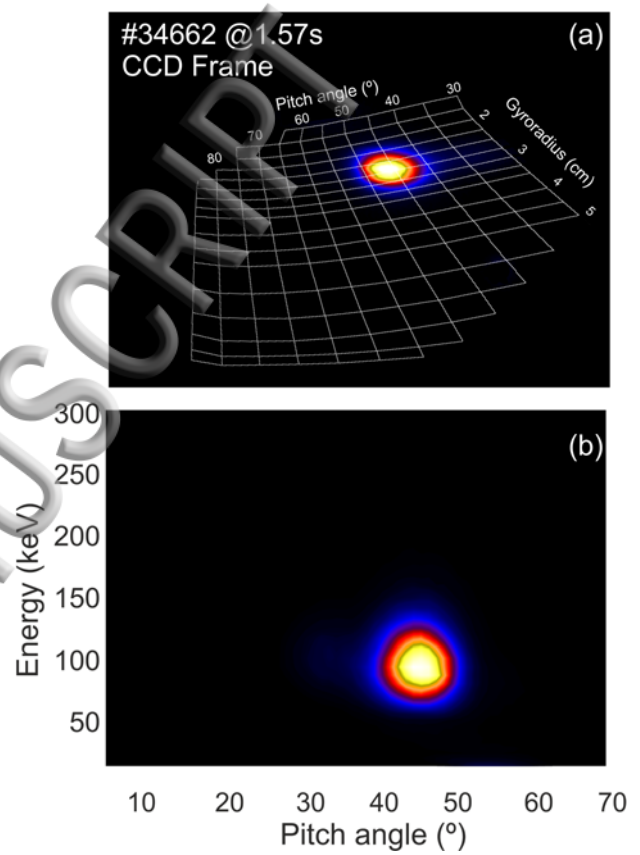

FIG. 7. a) Calculated strike map overlayered onto the CCD frame during first NBI blip. b) CCD frame triangulated according to strike map information and assuming deuterium ions.

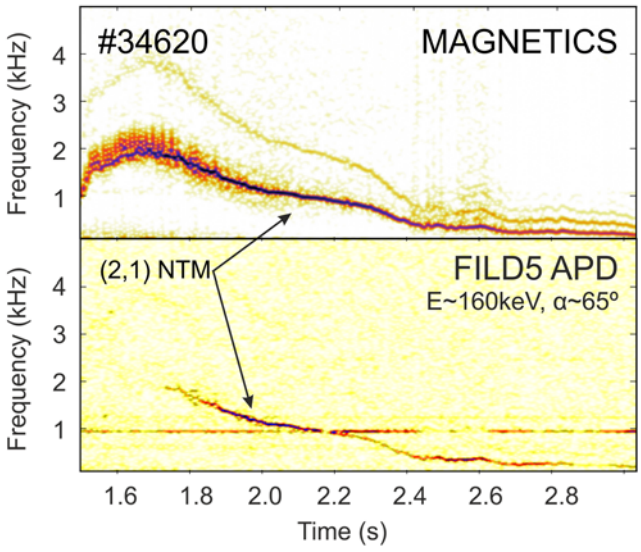

FIG. 8. Magnetic spectrogram showing a (2,1) magnetic island (top). FILD APD channel 57 spectrogram (bottom). (2,1) magnetic island is also observed in APD spectrogram, indicating MHD induced fast-ion losses.

IV. CONCLUSIONS AND FUTURE WORK

A new FILD has been designed, constructed and commissioned near the ASDEX Upgrade lower divertor. Due to its location, innovative features have been included such as off-axis reciprocating system, in-vessel movable lenses relay and coherent quartz image guide. PMTs have been replaced by an 8x8 channels APD camera for high temporal resolution measurements. During the last experimental campaign, NBI prompt losses and NTM induced fast-ion losses have been identified. This new detector improves the poloidal coverage of fast-ion losses on ASDEX Upgrade, which will be completed with the recently installed magnetically-driven FILD4[15].

ACKNOWLEDGMENTS

The authors would like to show their gratitude to Wolfgang Popken for his contribution to this project.
This work has been carried out within the framework of the EUROfusion Consortium and has received funding from the Euratom research and training programme 2014-2018 under Grant Agreement No. 633053. The views and opinions expressed herein do not necessarily reflect those of the European Commission.

[1]A. Fasoli *et al.* Nucl. Fusion **47**, S264 (2007).
[2]M. Garcia-Munoz, H.-U. Fahrbach and H.Zohm, Rev. Sci. Instrum. **80**, 53503 (2009).
[3]M. Garcia-Munoz *et al.*, Plasma Phys. Controlled Fusion, 55**,** 124014 (2013).
[4]X. Chen *et al.,* Rev. Sci. Instrum. **83**, 10D707 (2012).
[5]S. Baeumel *et al.,* Rev. Sci. Instrum. **75**, 3563 (2004)
[6]S. J. Zweben, R. L. Boivin, M. Diesso, S. Hayes, H. W. Hendel, H. Park and J. D. Strachan, Nucl. Fusion **30**, 1551 (1990).
[7]M.A. Van Zeeland *et al.,* Plasma Phys. Control. Fusion **56**, 015009 (2014).
[8]S.J. Zween, *et al.,* 'Recent progress on MHD-induced loss of D-D fusion products in TFTR'. (PPPL--2934) (1993).
[9]J. Ayllon-Guerola *et al.,* Rev. Sci. Instrum. (Submitted) (2018).
[10]I. Zammuto, M. Rott, B. Streibl, W. Suttrop and T. Vierle, Fusion. Eng. Des. **86**, 1067 (2011).
[11]P. de Marné, A. Herrmann and P. Leitenstern, Fusion Eng. Des. **123**, 754 (2017).
[12]G. Náfrádi, A. Kovácsik, G. Pór, M. Lampert, Y. Un-Nam and S. Zoletnik, Nuclear Instruments and Method in Physics Research, **770**, 21 (2015).
[13]E. Dunai, S. Zoletnik, J. Sárzközi, and A. R. Field, Rev. Sci. Instrum, **81**, 103503 (2010).
[14]J. Galdon-Quiroga *et al.,* 'Velocity-space sensitivity and tomography of scintillator-based fast-ion loss detectors', submitted to Plasma Physics and Controlled Fusion.
[15]J.Ayllon *et al.,* Rev. Sci. Instrum. **87**, 11E705 (2016).

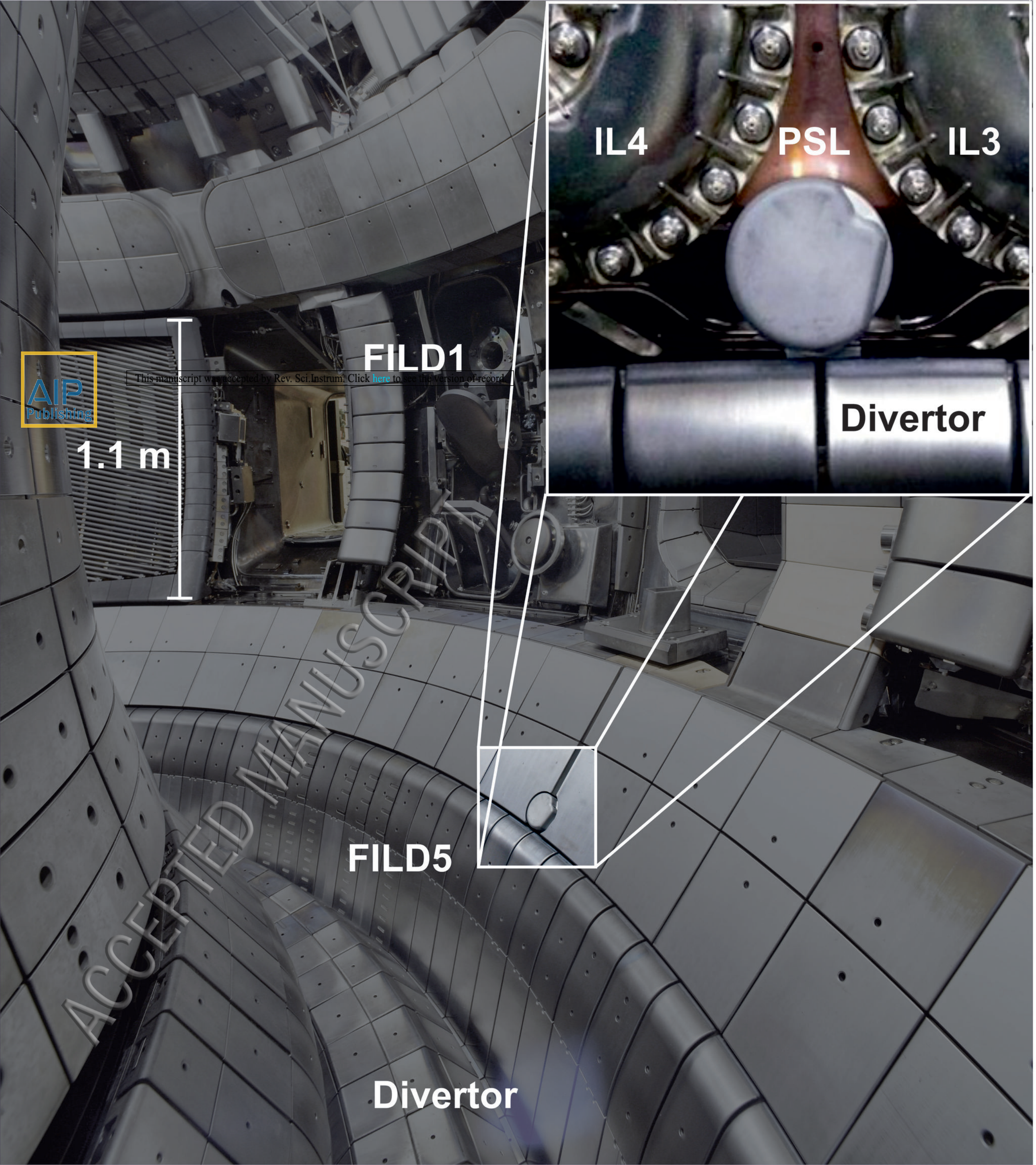

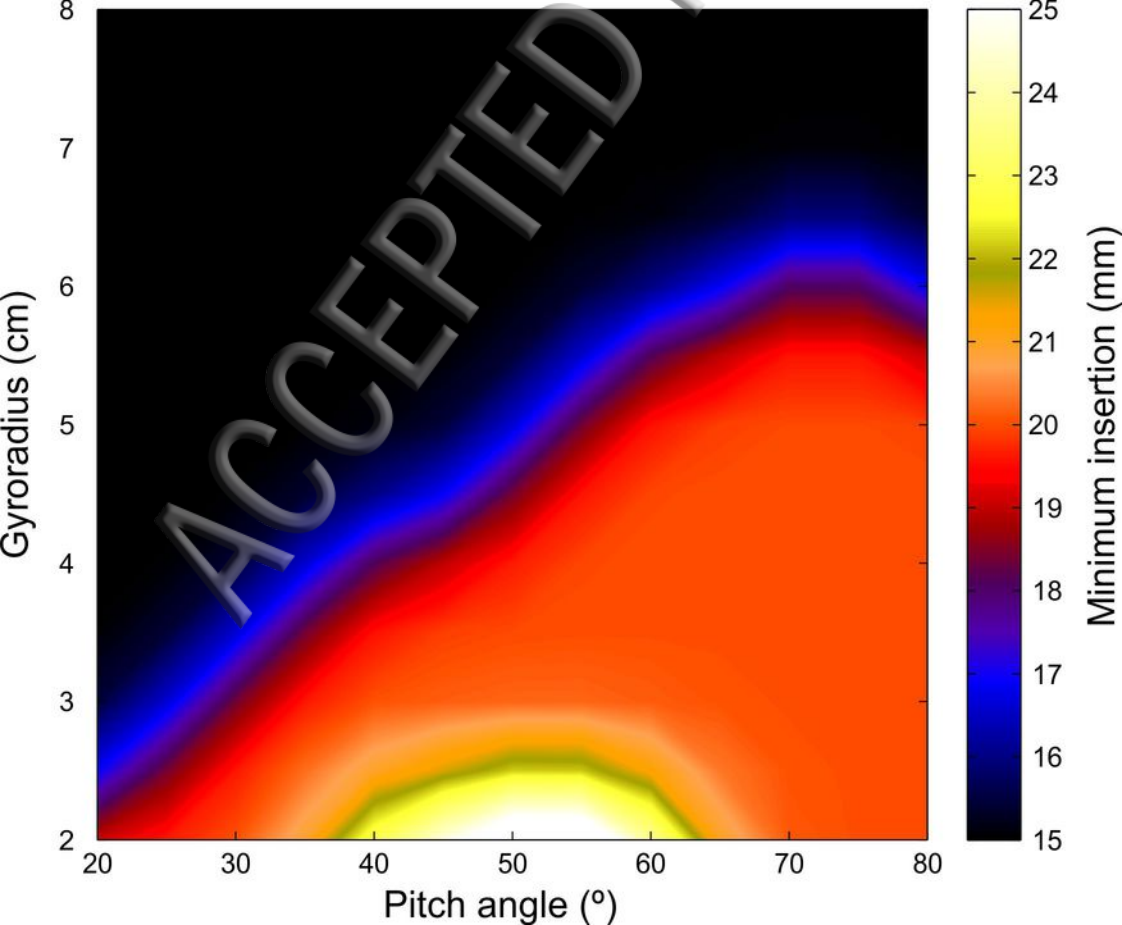
Gyroradius (cm)
8
7
6
5
4
3
2
20
30
40
50
60
70
80
Pitch angle (º)
Minimum insertion (mm)
25
24
23
22
21
20
19
18
17
16
15

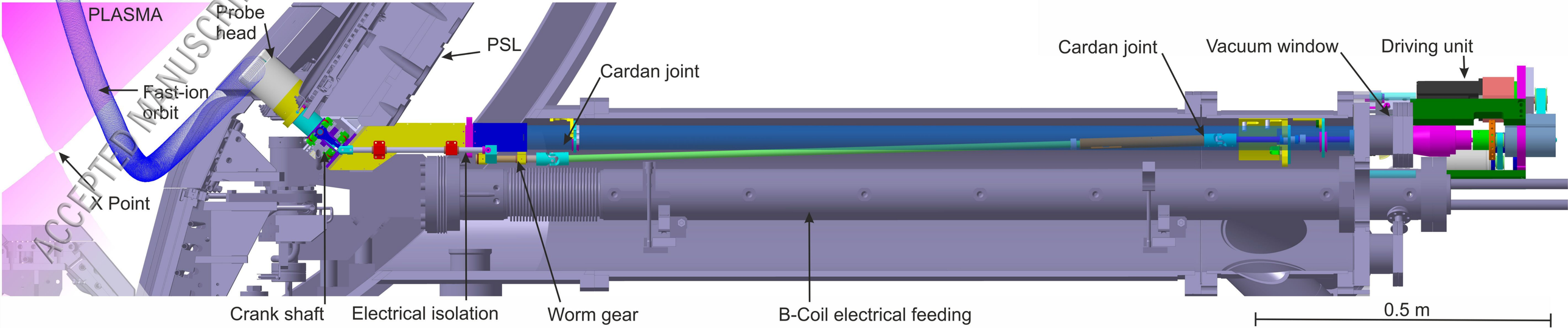

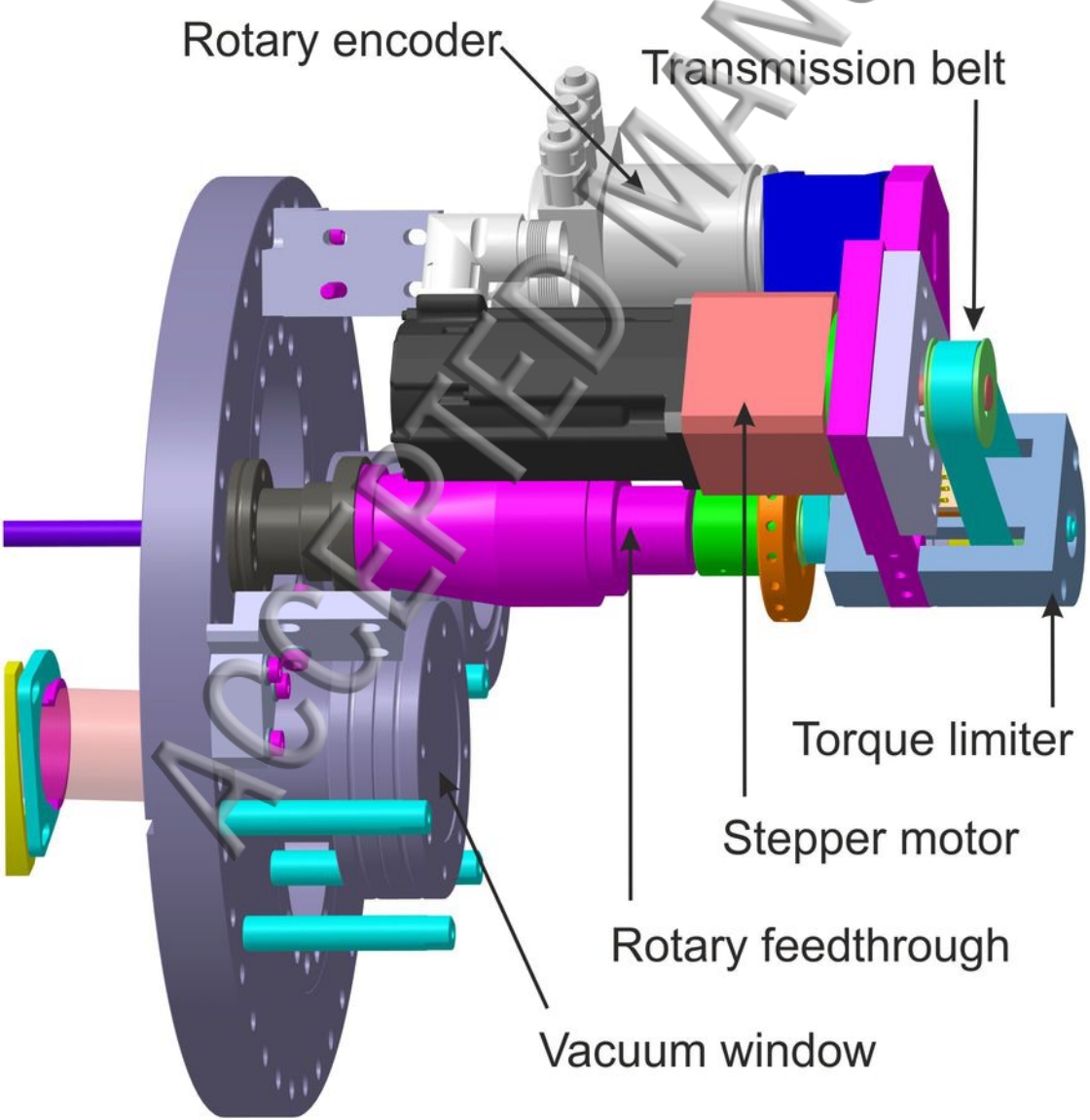

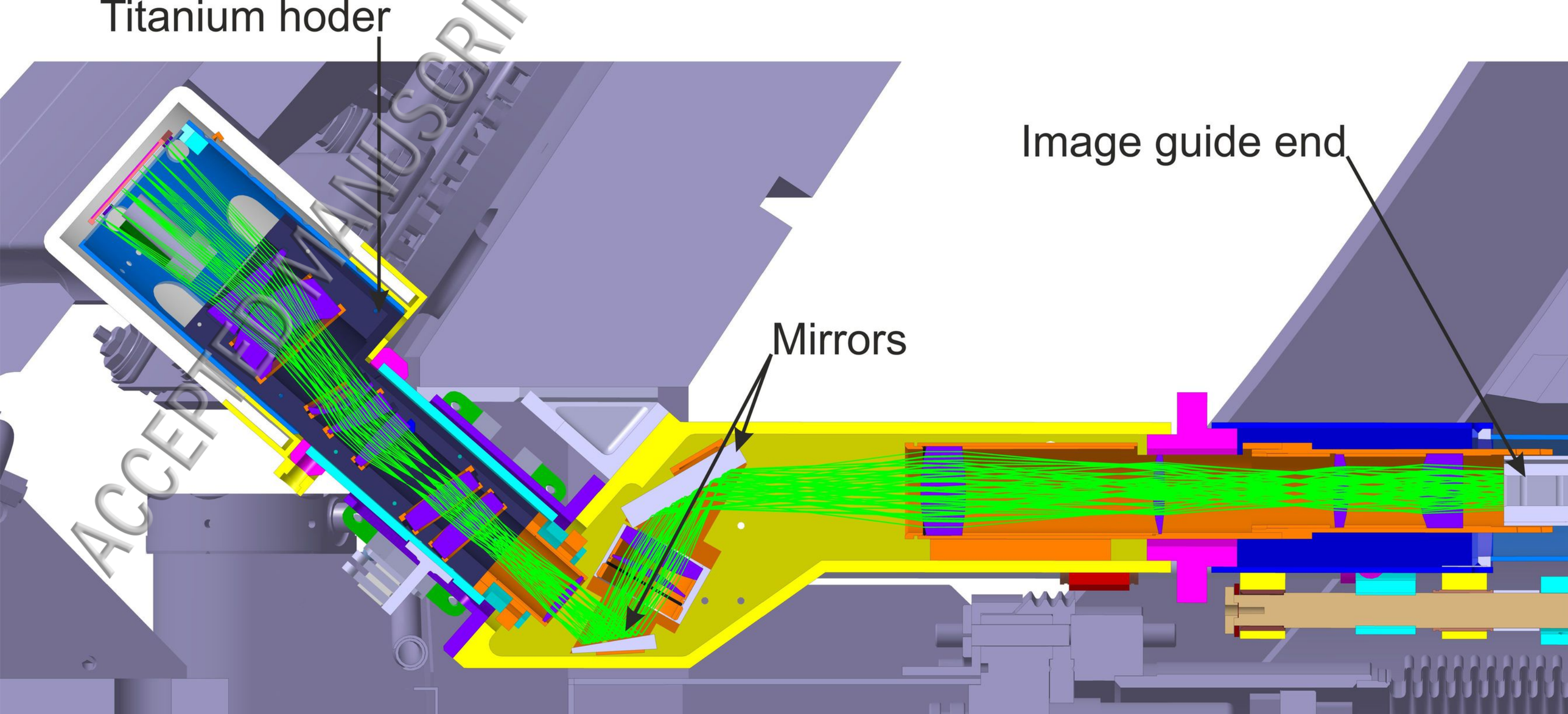
Titanium hoder
Image guide end
Mirrors

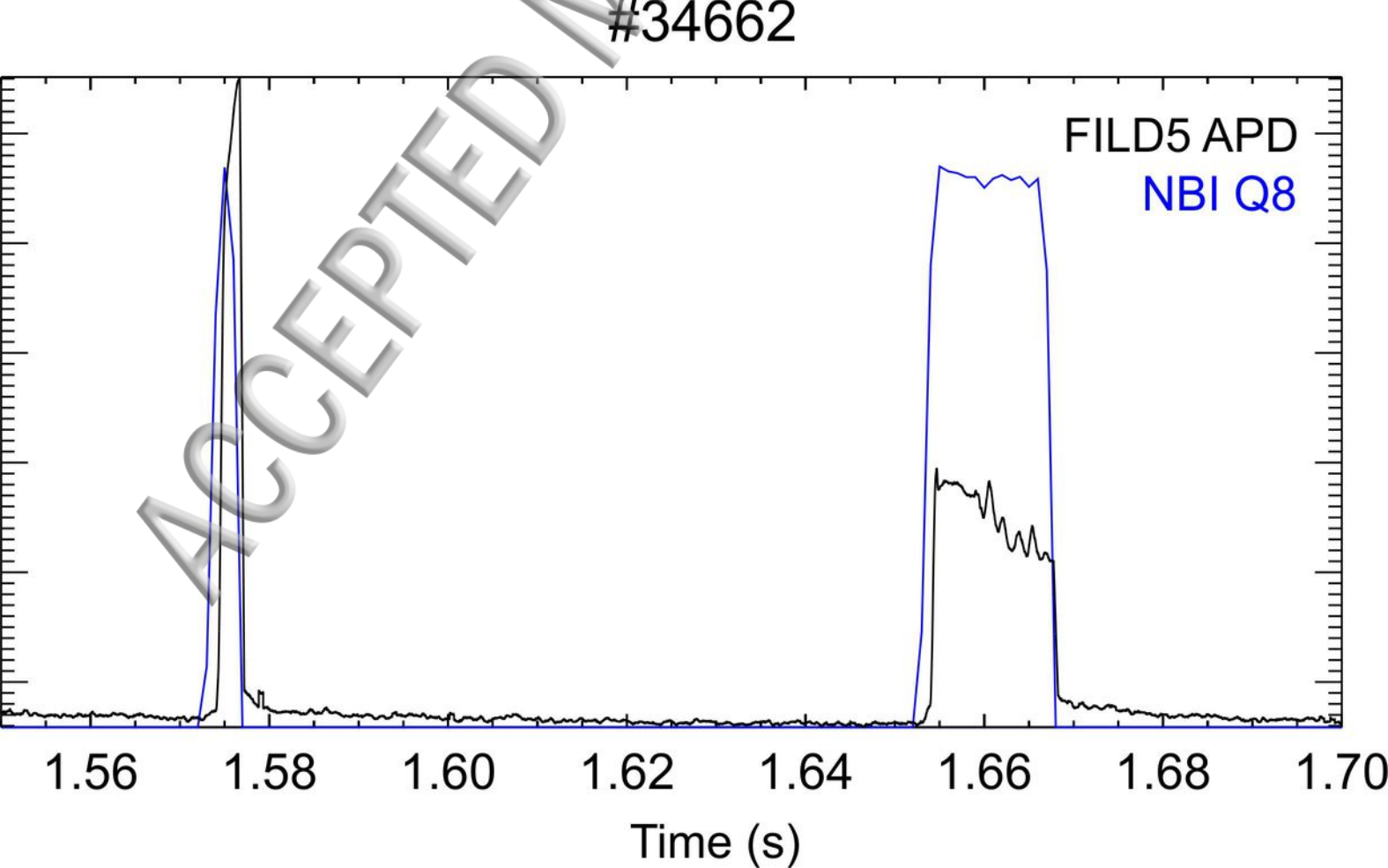

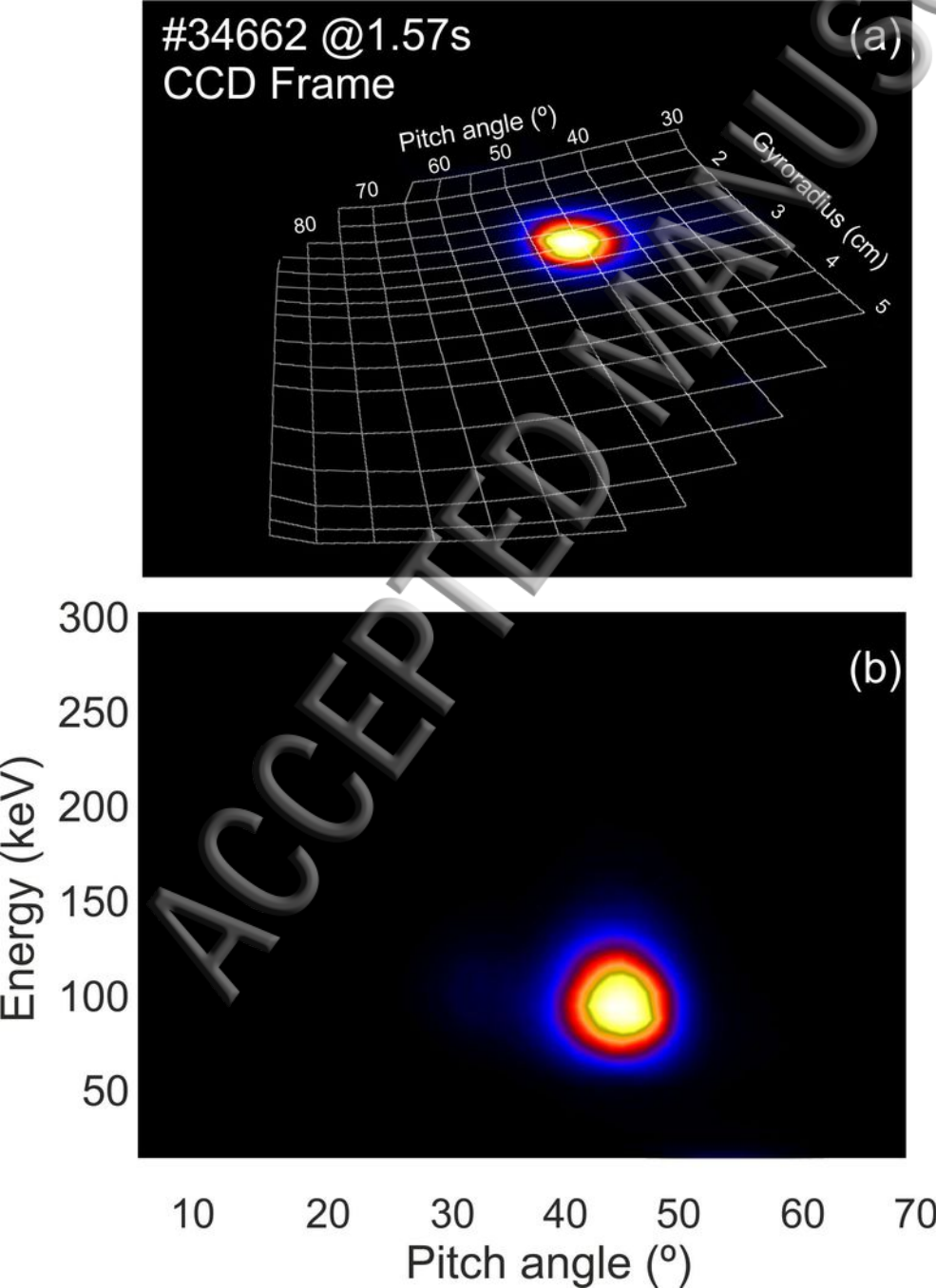

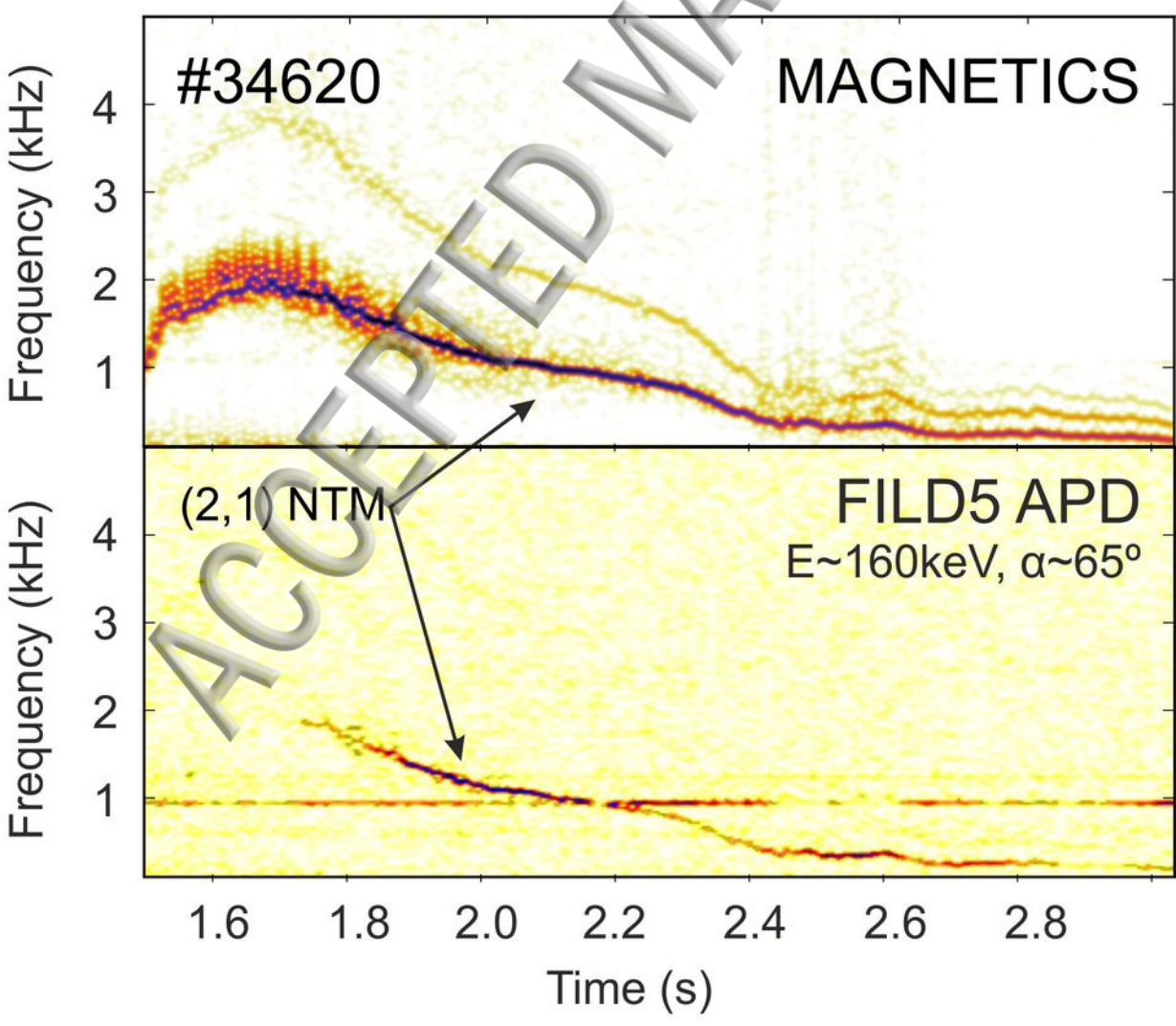
#34620
MAGNETICS
Frequency (kHz)
4
3
2
1
(2,1) NTM
FILD5 APD
E~160keV, α~65º
Frequency (kHz)
4
3
2
1
1.6
1.8
2.0
2.2
2.4
2.6
2.8
Time (s)